RMetS
Royal Meteorological Society

High-resolution temperature and precipitation projections over Ontario, Canada: a coupled dynamical-statistical approach

Xiuquan Wang,[a] Guohe Huang,[a,b]* Qianguo Lin,[c] Xianghui Nie[a] and Jinliang Liu[d]

[a]*Institute for Energy, Environment and Sustainable Communities, University of Regina, Saskatchewan, Canada*
[b]*SC Institute for Energy, Environment and Sustainability Research, North China Electric Power University, Beijing, China*
[c]*MOE Key Laboratory of Regional Energy and Environmental Systems Optimization, North China Electric Power University, Beijing, China*
[d]*Department of Earth and Space Science and Engineering, York University, Toronto, Ontario, Canada*

*Correspondence to: G. Huang, Institute for Energy, Environment and Sustainable Communities, University of Regina, Regina, Saskatchewan S4S 0A2, Canada. E-mail: huang@iseis.org

We develop a dynamical–statistical downscaling approach by coupling the PRECIS regional modelling system and a statistical method – SCADS – to construct very high resolution climate projections for studying climate change impacts at local scales. The coupled approach performs very well in hindcasting the mean temperature of present-day climate, while the performance for precipitation is relatively poor due to its high spatial variability and nonlinear nature but its spatial patterns are well captured. We then apply the coupled approach for projecting the future climate over the province of Ontario, Canada at a fine resolution of 10 km. The results show that there would be a significant warming trend throughout this century for the entire province while less precipitation is projected for most of the selected weather stations. The projections also demonstrate apparent spatial variability in the amount of precipitation but no noticeable changes are found in the spatial patterns.

Key Words: regional climate projection; dynamical downscaling; statistical downscaling; impacts studies

Received 17 March 2014; Revised 21 May 2014; Accepted 7 July 2014; Published online in Wiley Online Library

1. Introduction

Global climate models (GCMs) are widely used to project future climate under the Special Report on Emissions Scenarios (SRES; Nakićenović, 2000) or the representative concentration pathways (Van Vuuren *et al.*, 2011). Generally, GCMs run at the global scale with a coarse resolution of 150–300 km. Assessment of climate change impacts at regional scales usually requires future climate projections at a much finer resolution (in the order of 10 km). Over recent years, downscaling techniques have been developed in the climate research community (e.g. Semenov and Barrow, 1997; Wilby *et al.*, 2002; Jones, 2004; Pal *et al.*, 2007; Hessami *et al.*, 2008), with the purpose of bridging the gap in the spatial resolution between GCMs and impact models (e.g. for hydrology and agriculture).

The downscaling techniques are classified into two categories: dynamical downscaling and statistical downscaling (Hewitson and Crane, 1996). Dynamical downscaling is a nested regional climate modeling technique which usually consists of using initial conditions, time-dependent lateral meteorological conditions and surface boundary conditions derived from GCMs or reanalysis of observations to drive high-resolution regional climate models (RCMs; Giorgi *et al.*, 2001). RCMs are developed using the same laws of physics as described in GCMs to account for the sub-GCM grid-scale processes with more details (such as mountain ranges, coastal zones, and details of soil properties) in a physically based way (Feser *et al.*, 2011). Nesting RCMs into GCMs can lead to improved simulation of the general circulation and thus can provide projections for a variety of climate variables at fine spatial scales (Zhang *et al.*, 2006; Lavender and Walsh, 2011; White *et al.*, 2013; Wang *et al.*, 2014). The major challenge to the dynamical technique is that RCM simulations can be computationally expensive in practice, depending on the domain size, spatial resolution, as well as the simulation length. In comparison, statistical downscaling mainly involves the development of quantitative relationships between large-scale atmospheric variables (named predictors) and local surface variables such as temperature and precipitation (named predictands); this approach is easier to implement with much lower computation requirements (Wilby *et al.*, 2004). A large number of previous research practices have employed statistical techniques to assess climate change impacts at either point or catchment scales (e.g. Charles *et al.*, 2004; Fowler *et al.*, 2007; Timbal *et al.*, 2009; Mullan *et al.*, 2012). Nevertheless, statistical downscaling is subject to an unverifiable assumption that the statistical relationships developed for present-day climate should hold under different future climate forcing conditions.

Both dynamical and statistical downscaling techniques have their own advantages for generating fine-resolution climate projections at regional scales. However, previous studies have

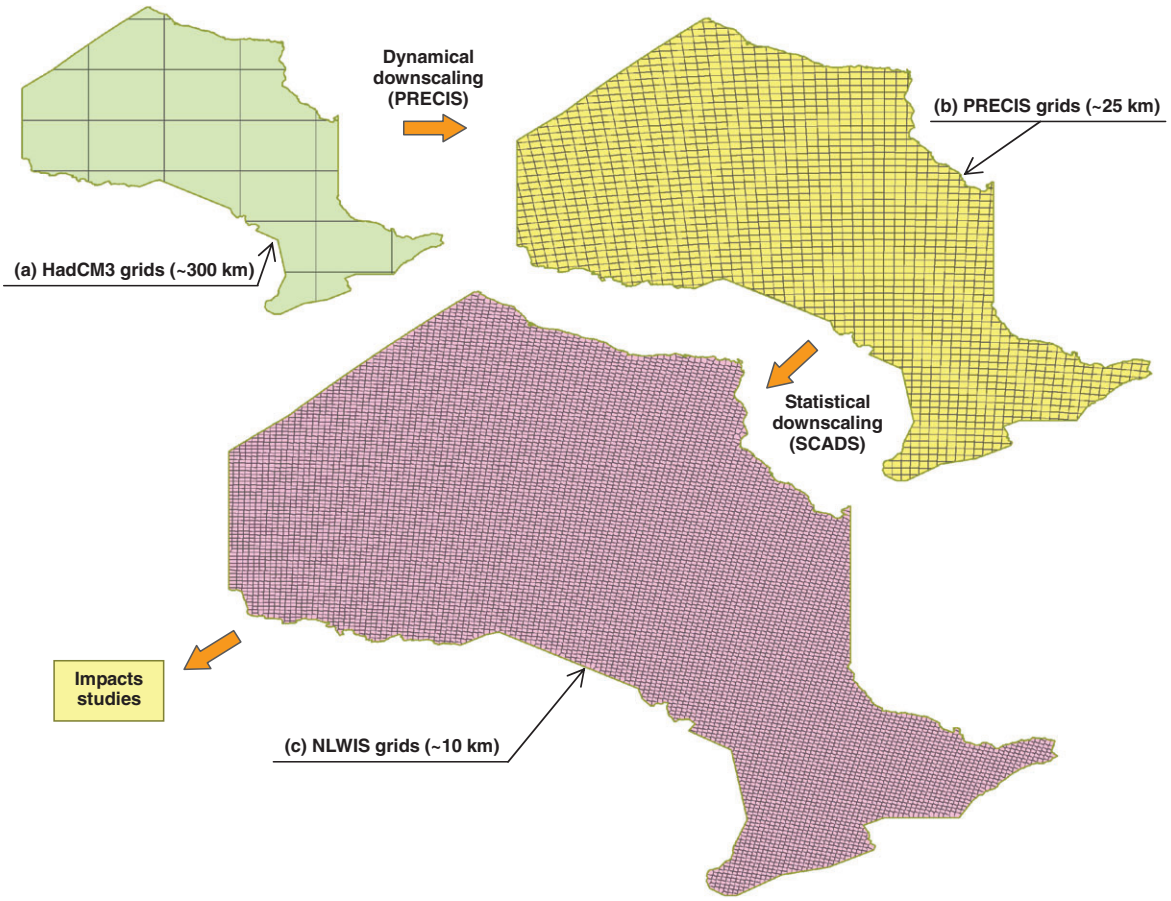

Figure 1. Illustration of the coupled dynamical–statistical downscaling approach used in this study.

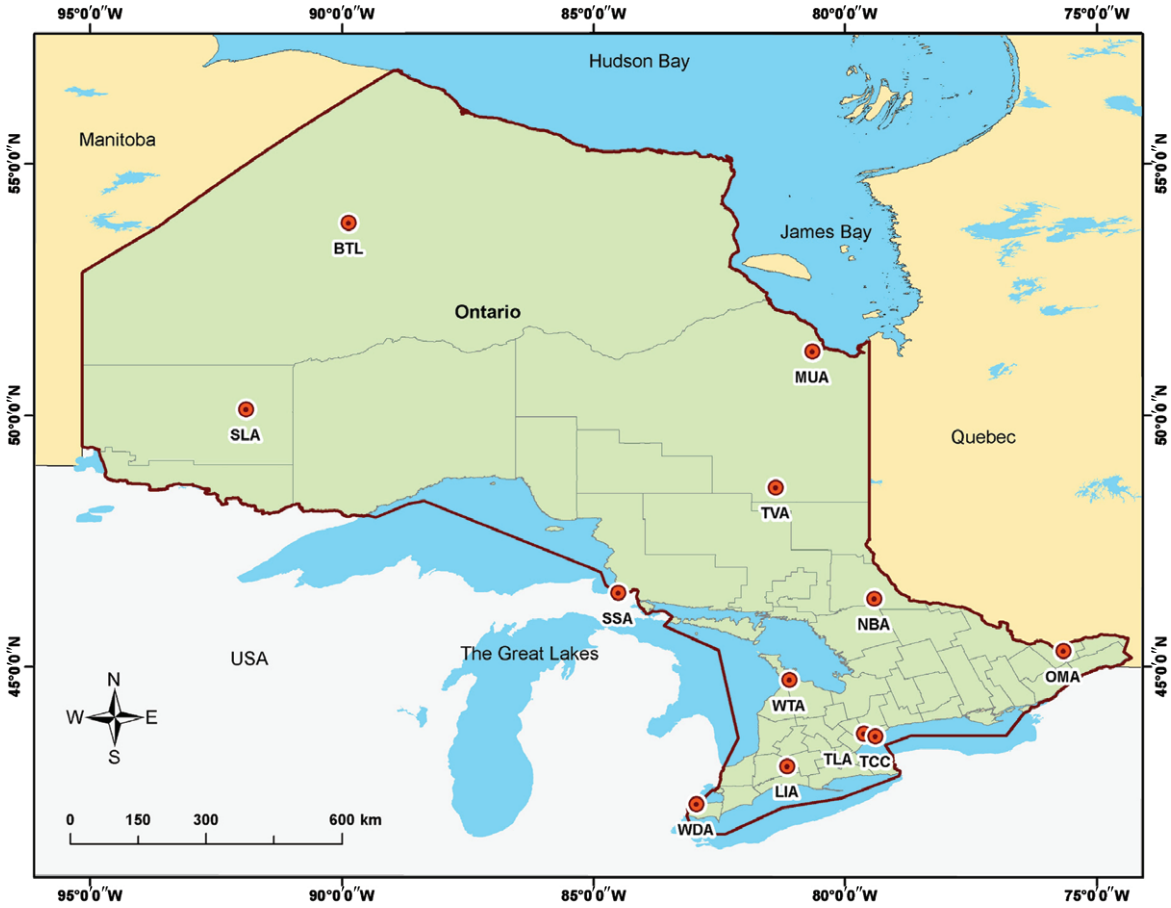

Figure 2. Locations of the 12 weather stations.

Table 1. Twelve weather stations selected in this study.

No.	Weather station	Longitude	Latitude	Abbreviation
001	Windsor Airport	82.96°W	42.28°N	WDA
002	London Int'l Airport	81.15°W	43.03°N	LIA
003	Toronto Lester B. Pearson Int'l Airport	79.63°W	43.68°N	TLA
004	Toronto City Center (Island Airport)	79.40°W	43.63°N	TCC
005	Ottawa Macdonald-Cartier Int'l Airport	75.67°W	45.32°N	OMA
006	Wiarton Airport	81.11°W	44.75°N	WTA
007	North Bay Airport	79.42°W	46.36°N	NBA
008	Sault Ste Marie Airport	84.51°W	46.48°N	SSA
009	Sioux Lookout Airport	91.90°W	50.12°N	SLA
010	Timmins Victor Power Airport	81.38°W	48.57°N	TVA
011	Big Trout Lake	89.87°W	53.83°N	BTL
012	Moosonee UA	80.65°W	51.27°N	MUA

Table 2. List of NARR variables selected as predictors for *Tmean* and *Precip*.

NARR variable	Unit	*Tmean*	*Precip*	NARR variable	Unit	*Tmean*	*Precip*
APCPsfc3h	kg m^{-2}	–	√	TMP30m	K	√	√
HGT500	gpm	√	–	UGRD500	m s^{-1}	√	–
HGT700	gpm	√	–	UGRD700	m s^{-1}	–	–
HGT850	gpm	√	–	UGRD850	m s^{-1}	–	–
HGT1000	gpm	–	√	UGRD1000	m s^{-1}	–	√
PRESsfc	Pa	–	√	UGRD10m	m s^{-1}	–	
PRES2m	Pa	√	√	UGRD30m	m s^{-1}	–	√
PRES10m	Pa	√	√	VGRD500	m s^{-1}	–	√
PRES30m	Pa	–	√	VGRD700	m s^{-1}	–	√
RH2m	%	√	√	VGRD850	m s^{-1}	–	√
SPFH500	kg kg^{-1}	√	–	VGRD1000	m s^{-1}	–	√
SPFH700	kg kg^{-1}	–	–	VGRD10m	m s^{-1}	√	√
SPFH850	kg kg^{-1}	–	–	VGRD30m	m s^{-1}	√	√
SPFH1000	kg kg^{-1}	√	√	VORT500	s^{-1}	–	–
SPFH2m	kg kg^{-1}	√	–	VORT700	s^{-1}	√	√
SPFH10m	kg kg^{-1}	√	–	VORT850	s^{-1}	–	√
SPFH30m	kg kg^{-1}	√	–	VORT1000	s^{-1}	√	√
TMP500	K	√	√	VORT10m	s^{-1}	√	√
TMP700	K	√	–	VORT30m	s^{-1}	√	√
TMP850	K	√	√	VVEL500	Pa s^{-1}	–	√
TMP1000	K	√	√	VVEL700	Pa s^{-1}	–	√
TMPsfc	K	√	√	VVEL850	Pa s^{-1}	–	√
TMP2m	K	√	√	VVEL1000	Pa s^{-1}	–	–
TMP10m	K	√	√				

'√' denotes that the indicated NARR variable was selected for predicting *Tmean* or *Precip*. The vorticity variables (i.e. VORT500, VORT700, VORT800, VORT1000, VORT10m, and VORT30m) are not direct outputs from the NARR dataset, but are calculated from eastward and northward wind components (Rhines, 1979).
APCPsfc3h = surface total 3 h precipitation; HGTxxx = geopotential height at xxx hPa; PRESxx = pressure at xx m; RH = relative humidity; SPFHxx = specific humidity; TMPxxx = temperature; UGRDxxx = eastward wind component; VGRDxx = northward wind component; VORTxxx = vorticity; VVELxxx = vertical pressure velocity.

been mostly focused on the application of a single technique (either dynamical or statistical downscaling) for climate change impact studies. One interesting question to be answered is whether or not the downscaled projections can be improved by coupling these two techniques into a general framework, instead of using either of them separately, and if so, by how much. Recently, a few studies have attempted to investigate the potential improvements through coupled dynamical–statistical or statistical–dynamical approaches (Hellström and Chen, 2003; Diez *et al.*, 2005; Chen *et al.*, 2012), and it was reported that the coupled approaches can improve the downscaled results to varying degrees.

Therefore, this study will focus on developing a dynamical–statistical downscaling approach by coupling a regional modeling system, Providing REgional Climates for Impacts Studies (PRECIS; Jones, 2004), and a statistical downscaling method, Stepwise Cluster Analysis Downscaling (SCADS; Wang *et al.*, 2013), to construct high-resolution climate projections for the province of Ontario, Canada. We first project the future climate of Ontario using the PRECIS model at its highest spatial resolution of 25 km. The SCADS model is then developed and validated at grid-point scale with a finer resolution of 10 km. We will show in the validation results that the SCADS demonstrates good performance in downscaling temperature and poor but acceptable performance in precipitation. We then apply the validated SCADS model to further downscale the projections generated by the PRECIS model. Finally, we will analyze the temporal trends and changes in the spatial patterns of both temperature and precipitation based on the high-resolution climate projections.

2. Data and methods

A coupled dynamical–statistical downscaling approach, as shown in Figure 1, was developed in this study to generate high-resolution climate projections. We first employed the well-known regional climate model PRECIS, which was developed at the UK Met Office Hadley Centre, to develop fine-scale physically based climate projections over the province of Ontario, Canada, by adding regionalized climate physics to the large-scale outputs from the HadCM3 modelling system under the SRES A1B emission scenario. The PRECIS model can be applied easily to any area of the globe to generate detailed climate change projections, with the provision of a simple user interface and a visualization and data-processing package (Jones, 2004; Wilson *et al.*, 2011). The PRECIS is able to run at two different horizontal resolutions: $0.44 \times 0.44^\circ$ (approximately 50×50 km^2) and $0.22 \times 0.22^\circ$ (approximately 25×25 km^2), with 19 atmospheric levels in the vertical using a hybrid coordinate system. In this study, the PRECIS was run at its highest resolution (i.e. 25 km) from 1950 to 2099 with the purpose of providing full simulations for both present-day and future climate.

To estimate regional climate details at even higher resolution, the stepwise cluster analysis downscaling method SCADS, developed by Wang *et al.* (2013), was then applied for further downscaling the 25 km physically based projections from PRECIS to a finer resolution of 10 km. Differing from the conventional downscaling methods, for example, the statistical downscaling model (SDSM; Wilby *et al.*, 2002) and automated statistical downscaling (ASD; Hessami *et al.*, 2008), the SCADS uses a cluster tree instead of a regression-based function to represent the complex relationships between large-scale predictors and local predictands. The cluster tree is constructed through a series of cutting and merging operations to a training sample set in a step-by-step fashion, which usually contains a large number of leaf nodes. Each leaf node in the cluster tree denotes a sub-cluster within the sample set, which cannot be further divided or merged with other sub-clusters. The prediction process for a given set of predictors is in fact a searching process starting from the top of the tree and ending at a leaf node, following a flow path guided by the cutting and merging rules; then the mean value or an interval bounded by the maximum and minimum values of the sample set in the leaf node can be used to estimate the corresponding predictand's value. The methodology and downscaling process of SCADS were detailed in the work of Wang *et al.* (2013).

To develop the SCADS model at grid-point scale, we derived 32 km reanalysis climate data covering the period 1979–2010 from the North American Regional Reanalysis (NARR) dataset produced by the National Centers for Environmental Prediction (NCEP). The NARR dataset was developed by using the very high resolution NCEP Eta Model together with the Regional Data Assimilation System (RDAS) which assimilated temperature, wind, precipitation, and many other variables (Mesinger *et al.*, 2006; Saha *et al.*, 2010). According to recommendations in the existing literature, we firstly screened out a number of predictor variables from the NARR dataset for predicting daily mean temperature and total precipitation (denoted as *Tmean* and *Precip*). For *Tmean*, the potential predictors may contain

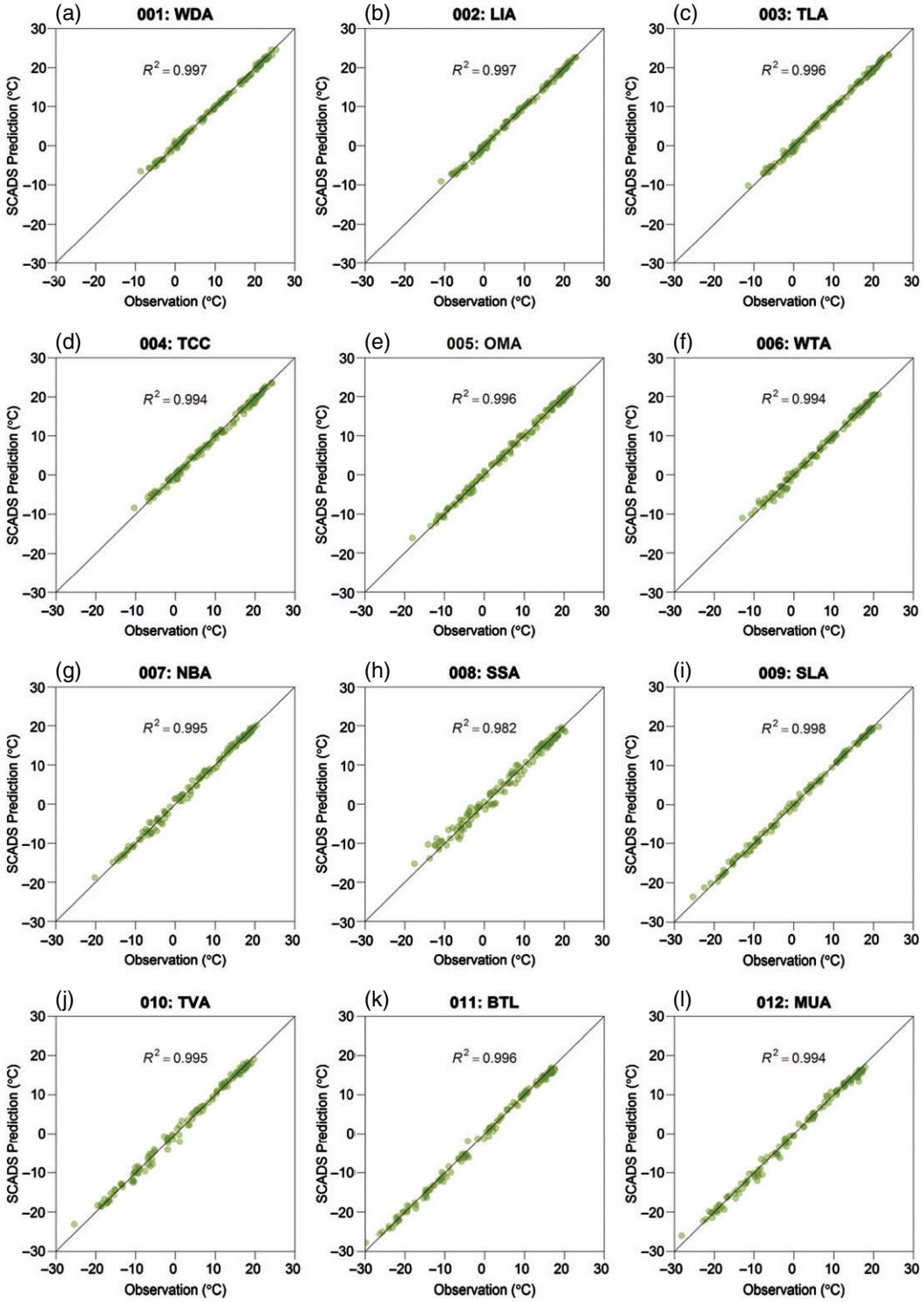

Figure 3. Validation results for monthly mean temperature at 12 weather stations. The coefficient of determination (R^2), ranging from 0 to 1, is calculated as a quantitative indicator to evaluate the performance of the SCADS model in reproducing observations.

500 hPa geopotential heights, surface air pressure, 850 hPa temperature, and 1000–500 hPa thickness (Crane and Hewitson, 1998; Huth, 1999; Wilby and Wigley, 2000; Hellstrom *et al.*, 2001; Chen and Chen, 2003); for *Precip*, the potential predictors may include surface air pressure, temperature, humidity, and upper-air measures of wind speed and direction, vorticity, divergence, humidity, temperature, and geopotential height (Beckmann and Adri Buishand, 2002; Salathé, 2003; Zhu *et al.*, 2005; Haylock *et al.*, 2006). The preliminary predictor set was further refined based on correlation analyses at 12 weather stations which are spatially distributed across Ontario (Figure 2 and Table 1). Finally, we chose different sets of predictors from the NARR datasets for predicting *Tmean* and *Precip* (Table 2).

High-resolution perdictand samples for both *Tmean* and *Precip* were collected from the 10 km gridded climate dataset (1961–2003) provided by the National Land and Water Information Service (NLWIS), Agriculture and Agri-Food, Canada. The NLWIS dataset was interpolated from daily Environment Canada climate station observations through a thin plate smoothing spline surface-fitting method as implemented by ANUSPLIN v4.3 (NLWIS, 2008). Due to the mismatch in time span, only a subset of the above two datasets covering the overlap period (i.e. 1979–2003) was extracted for statistical modelling in this study. In detail, the data for 1979–1993 were treated as the sample set to train the SCADS model. Based upon the work of Wang *et al.* (2013), we fixed the significance level as 0.05 during the training process because the calibration

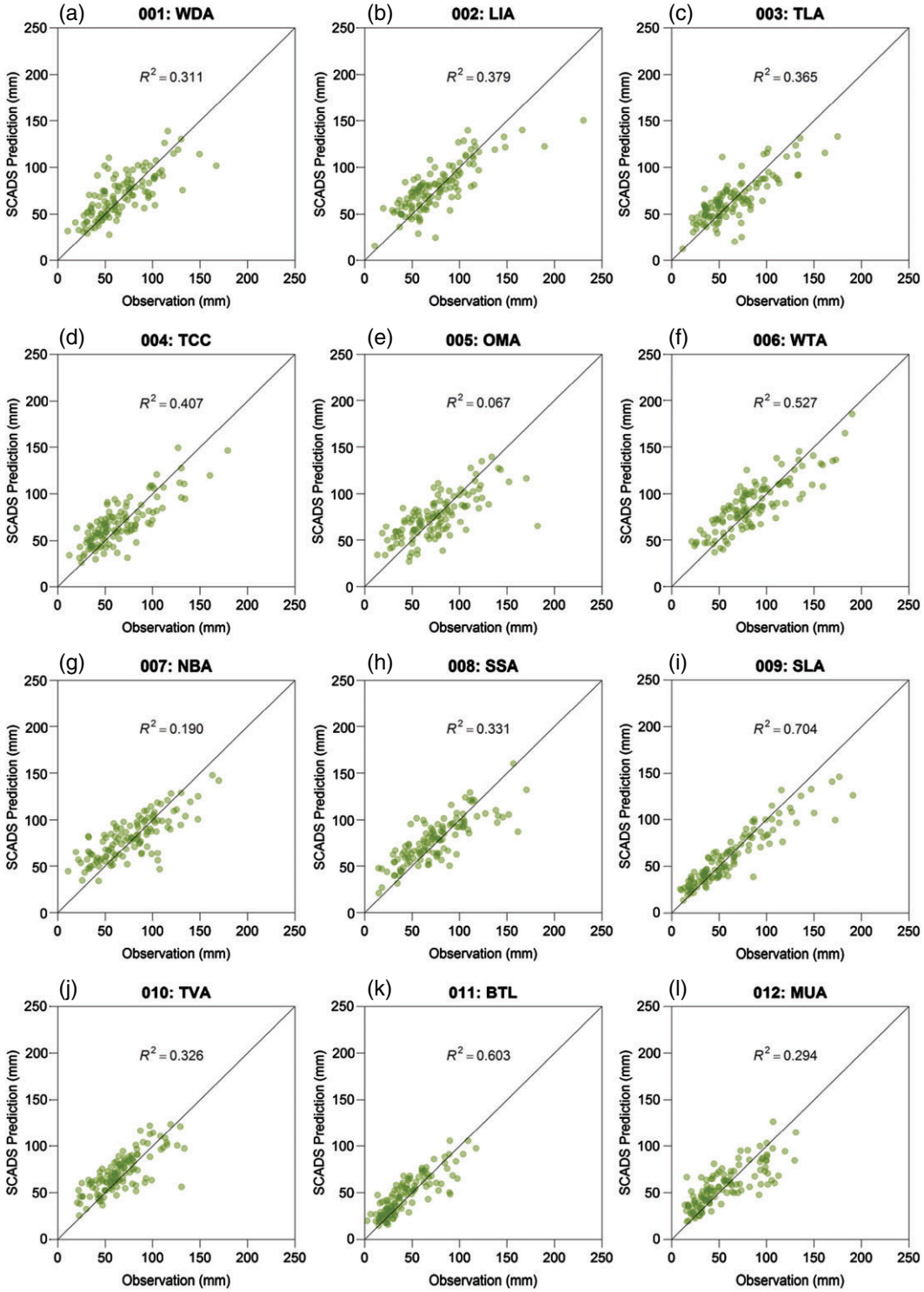

Figure 4. As Figure 3, but for monthly total precipitation.

results were insensitive to different significance levels ranging from 0.01 to 0.05. Thus a cluster tree reflecting the inherent relationship between regional coarse-resolution predictors and local high-resolution predictands can be established for each grid cell. The remaining ten-year data from 1994 to 2003 were used for validating the model performance at the 12 weather stations. Following that, the SCADS model was applied for statistically downscaling the PRECIS outputs to generate high-resolution climate projections for Ontario.

To analyze the temporal trends of climate projections generated from the coupled approach, We first employed the Locally Weighted Scatterplot Smoothing method (LOWESS; Cleveland, 1979) to smoothly fit the monthly time series of each station. The LOWESS algorithm is an outlier-resistant method based on local polynomial fits and thus is robust to reflect the overall trend of the time series. We then used the seasonal Kendall test (Mann, 1945; Kendall, 1970; Hirsch *et al.*, 1982) to test whether a significant trend existed in the time series under a given significance level (here we set $\alpha = 0.05$). The significance of the trend is quantified as the *P*-value. The Sen's slope estimator (Sen, 1968) is further applied to estimate the magnitude of the trend only if it is detected as significant. Positive values from the slope estimator indicate increasing trends while negative values represent decreasing ones.

3. Results

The validation results for monthly mean temperature and monthly total precipitation at the 12 weather stations are shown in Figures 3 and 4. The SCADS model demonstrates consistently

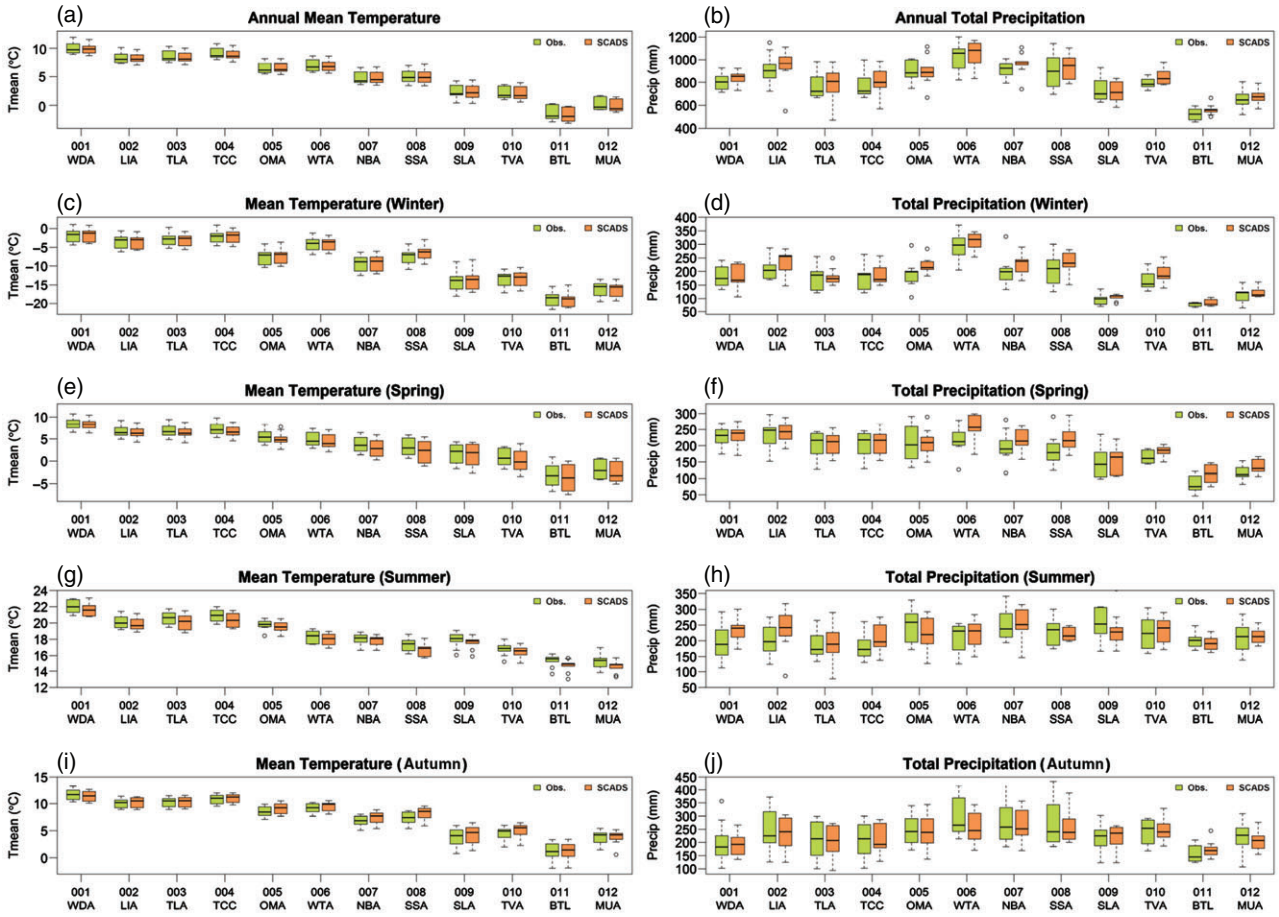

Figure 5. Comparisons of mean temperature and total precipitation for annual and seasonal time-scales at 12 weather stations. (Winter = December of the previous year, January, and February; spring = March, April, and May; summer = June, July, and August; autumn = September, October, and November).

outstanding performance in terms of reproducing monthly mean temperature at the 12 weather stations, with the lowest R^2 value being as high as 0.982 at the SSA station. However, the performance of SCADS for precipitation is not as good as that for temperature. The R^2 values for precipitation vary greatly at the 12 stations and show evident spatial variability. The highest R^2 value is achieved at the SLA station (0.704), while the lowest one is obtained at the OMA station (0.067). Nevertheless, the R^2 values at most stations are still greater than 0.3 which leads to an averaged R^2 value of 0.375. This indicates the overall performance of SCADS is acceptable in the downscaling practice since precipitation is considerably more difficult to model than temperature due to its high spatial variability and its nonlinear nature (Maraun *et al.*, 2010). In addition, the performance of SCADS model is further investigated by comparing box plots of mean temperature and total precipitation for annual and seasonal time-scales between the SCADS outputs and the observations (Figure 5). The central estimates and mass distributions for mean temperature at all stations are well simulated by the SCADS model, further affirming its good performance for temperature. By contrast, the SCADS model shows a relatively poor capability to reproduce the current observed precipitation for both annual and seasonal time-scales. Although the SCADS model produces either higher or lower estimates relative to the observations at some stations (e.g. higher annual total precipitation at the NBA station, lower summer precipitation at the OMA station), the overall spatial patterns of precipitation at the 12 weather stations are still well captured.

We obtained 10 km high-resolution climate projections for Ontario by further downscaling the 25 km outputs from PRECIS with the validated SCDAS model. Trend analyses were then carried out at the 12 weather stations to help understand how the future temperature and precipitation over Ontario are likely to change under the SRES A1B emission scenario. Figure 6 shows the projected trends of monthly mean temperature at the 12 weather stations. It is quite clear that all stations consistently present significant warming trends, with all of the P-values less than 0.001 and the trends ranging from 0.004 to 0.005 °C per month. The projected trends of monthly total precipitation are shown in Figure 7. Unlike temperature, the trend of precipitation at each station tells a different story due to its spatial variability. Even though some stations show similar trends, e.g. the monthly precipitation at the stations WDA, TLA, OMA, and NBA are projected to be decreasing by ∼0.008 mm per month, their temporal patterns vary greatly. Note that the temporal pattern here is referred to as the range of monthly total precipitation as well as its fluctuation over time. For example, the projected monthly total precipitation at WTA mostly ranges between 50 and 300 mm and its fluctuation is likely to decrease to the end of this century, while the precipitation at NBA mostly varies between 20 and 100 mm and its fluctuation tends to be increase with time. Thus, these two stations show different temporal patterns. As shown in Figure 7, there are no significant trends detected at SLA, BTL, and MUA, while the remaining stations show similar decreasing trends with the slope fluctuating between 0.005 and 0.017 mm per month. Furthermore, the time series of temperature and precipitation for annual and seasonal time-scales at the 12 weather stations are plotted (Figure 8) to understand their temporal patterns and trends from the near term to the end of this century. The plots for annual and seasonal mean temperature present similar patterns and further confirm the significant warming trends for all stations, while the plots for precipitation show different temporal patterns at all stations and most of the stations reveal to different degrees decreasing trends in the amount of precipitation.

The high-resolution projections for temperature and precipitation were then divided into three 30-year periods: 2010–2039 (2020s), 2040–2069 (2050s), and 2070–2099 (2080s), to further

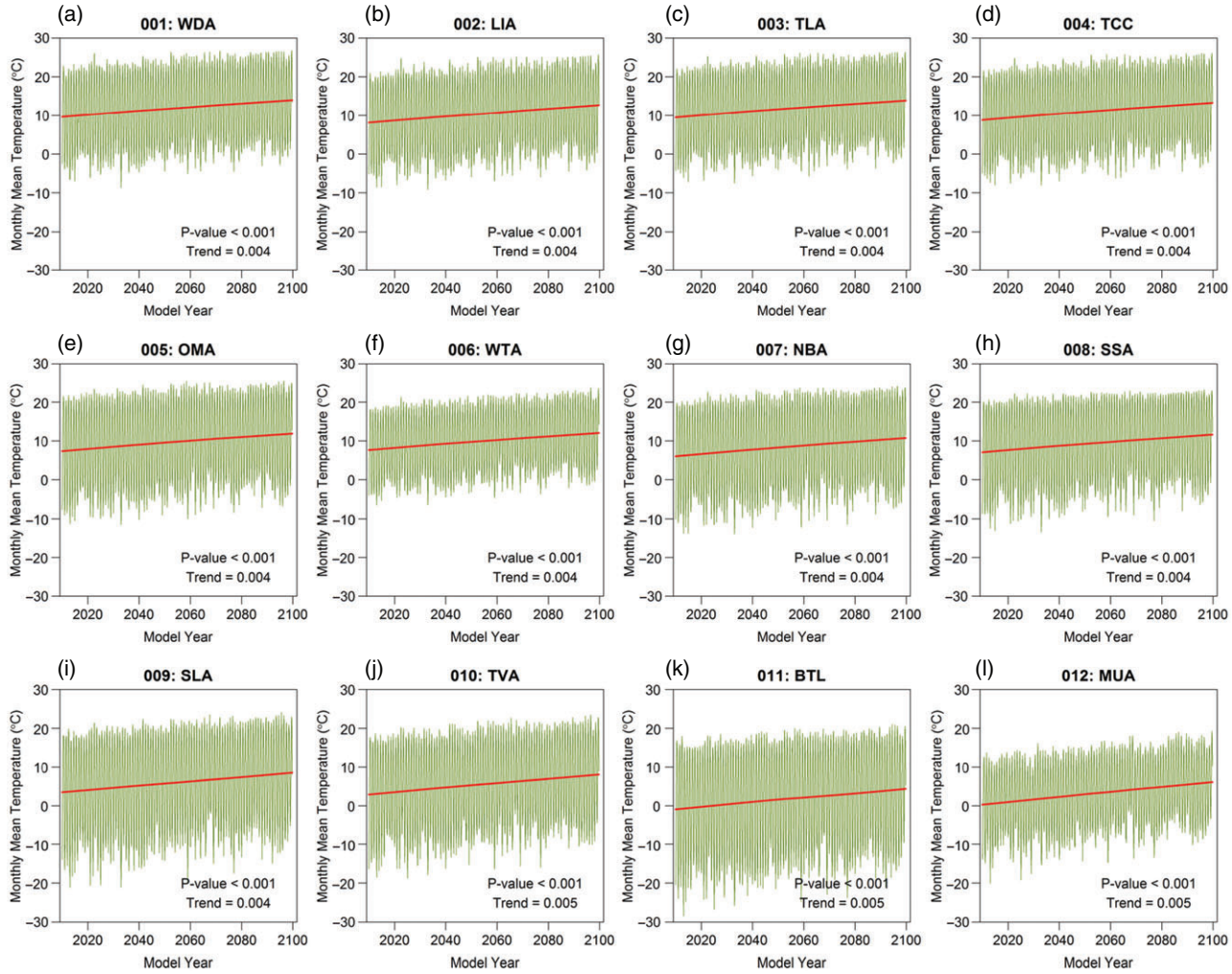

Figure 6. Trends of projected monthly mean temperature at 12 weather stations (Figure 2) from 2010 to 2099. The smoothed lines for the time series are fitted using the LOWESS method. A non-parametric statistical test, the seasonal Kendall test, is used to determine the significance of a trend in the time series (denoted as *P*-value), and Sen's slope estimator is used to estimate the magnitude of the trend (expressed as °C per month).

analyze their near-term and long-term spatial patterns over the entire province of Ontario. Figure 9 shows the maps of projected annual mean temperature and total precipitation over Ontario for the three periods. The maps for temperature reveal an obvious increasing trend from the 2020s to 2080s across the entire province. The mean temperature of north Ontario would rise from (−3 to 0) °C in the 2020s to (−1 to 2) °C in the 2050s, and then to as high as (1 to 4) °C in the 2080s, while the mean temperature of south Ontario would jump from (7 to 10) °C in the 2020s to (11 to 14) °C in the 2080s. The projected warming trend is likely to drive the annual mean temperature of Ontario up to (6 to 8) °C by the end of this century. It is interesting that there are no significant changes in the spatial patterns of precipitation from the 2020s to 2080s. However, the spatial variability of precipitation is clearly reflected in the projected maps. The highest spots of precipitation are mostly distributed in the west and southeast regions where the annual total precipitation would be as high as 2400 mm, while lower precipitation is projected in the northern area where the annual precipitation would be as low as 400 mm.

4. Summary and conclusions

Previous studies have showed that the downscaling performance can be improved through coupled approaches (Chen *et al.*, 2012). In this study, we further investigated the improved performance by developing a coupled dynamical–statistical downscaling approach, which integrates the PRECIS regional model system and a new statistical method SCADS into a general framework, to help generate very high resolution climate projections for the province of Ontario, Canada. By validating the downscaled results at 12 weather stations across Ontario, we showed that the coupled approach can reproduce the observed temperature of current climate very well, while the performance for precipitation was relatively poor but still acceptable and its spatial patterns were primarily captured also.

We then applied the coupled approach for generating 10 km high-resolution climate projections. By analyzing the trends and spatial patterns of projected temperature and precipitation, we found that there would be a significant warming trend throughout this century for the province of Ontario. Such a continuous increasing trend is likely to raise the mean temperature of Ontario to (6 to 8) °C by the end of this century. Meanwhile, the projected precipitation at most of the weather stations showed decreasing trends to varying degrees. The results also disclosed apparent spatial variability in the amount of precipitation but no evidence for the changes in the spatial patterns of precipitation was found.

Overall, the coupled downscaling approach demonstrated good performance in generating high-resolution climate projections by combining the advantages of both dynamical and statistical techniques. However, the major drawback of this approach is that the effects of systematic errors in the driving fields provided by GCMs would be transferred into the downscaled projections via a two-step process (first into RCMs and then into statistical models). Further research is desirable to investigate the effects of the transferred errors on the improved performance within a coupled framework.

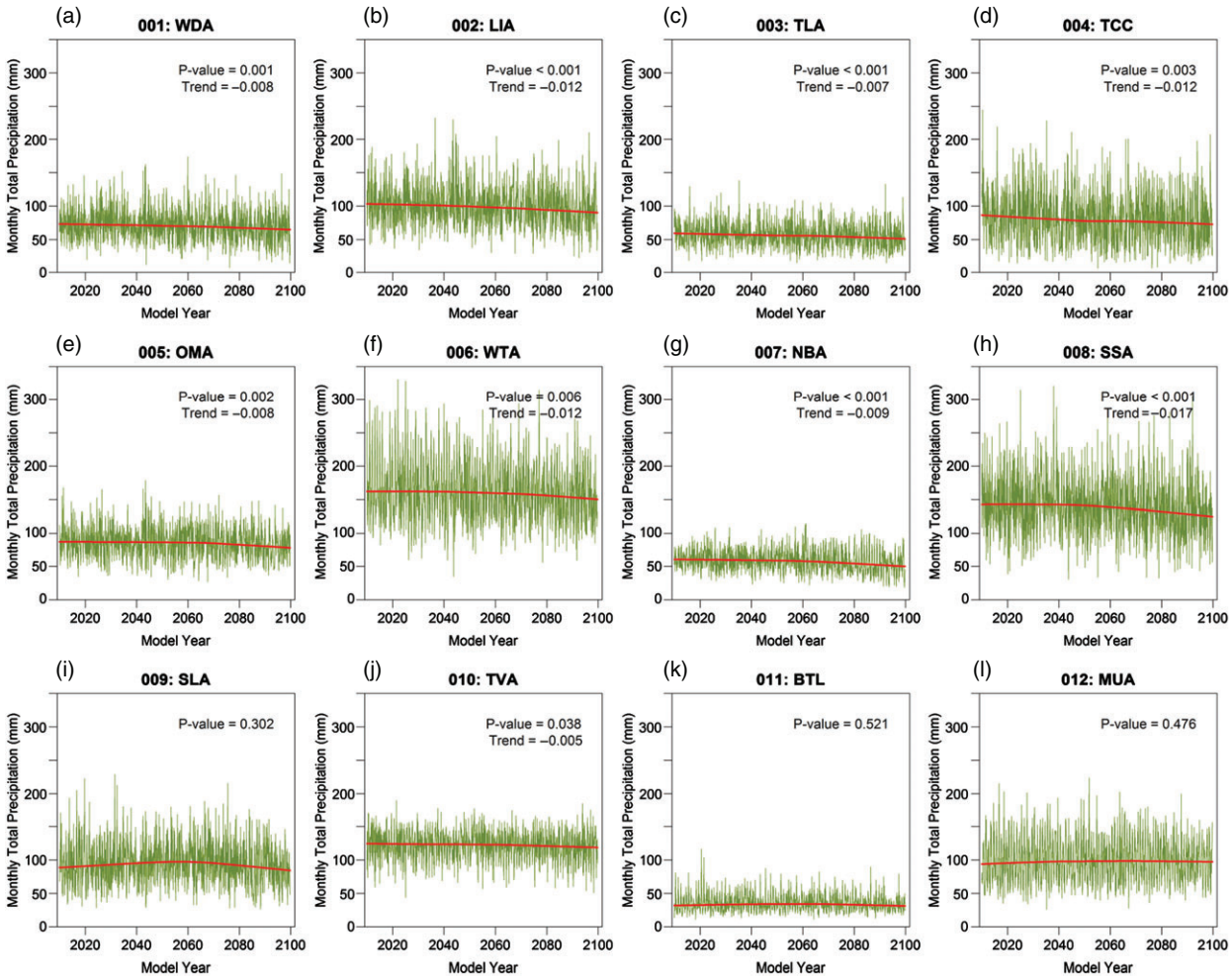

Figure 7. As Figure 6, but for projected monthly total precipitation. The trend here is expressed as mm per month.

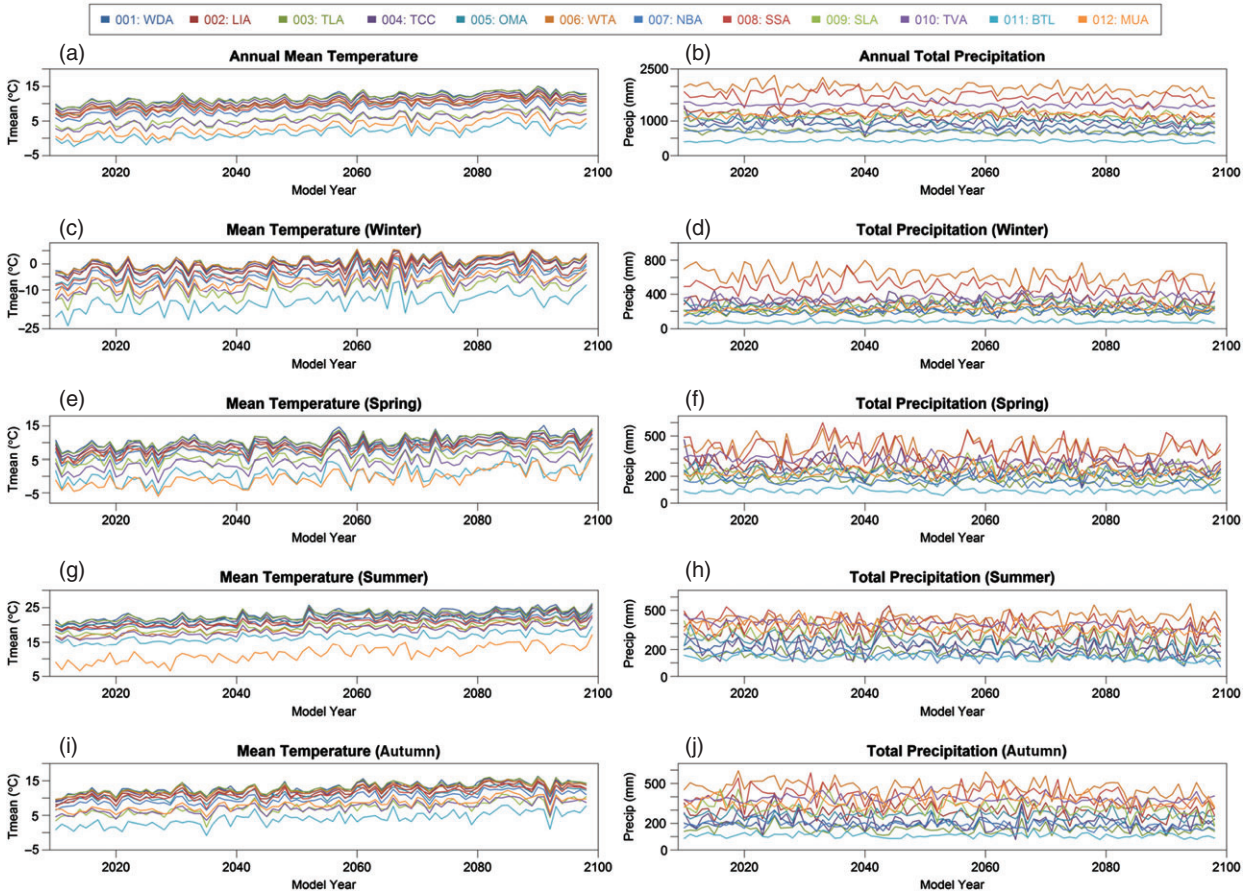

Figure 8. Time series of projected mean temperature and total precipitation for annual and seasonal time-scales at the 12 weather stations.

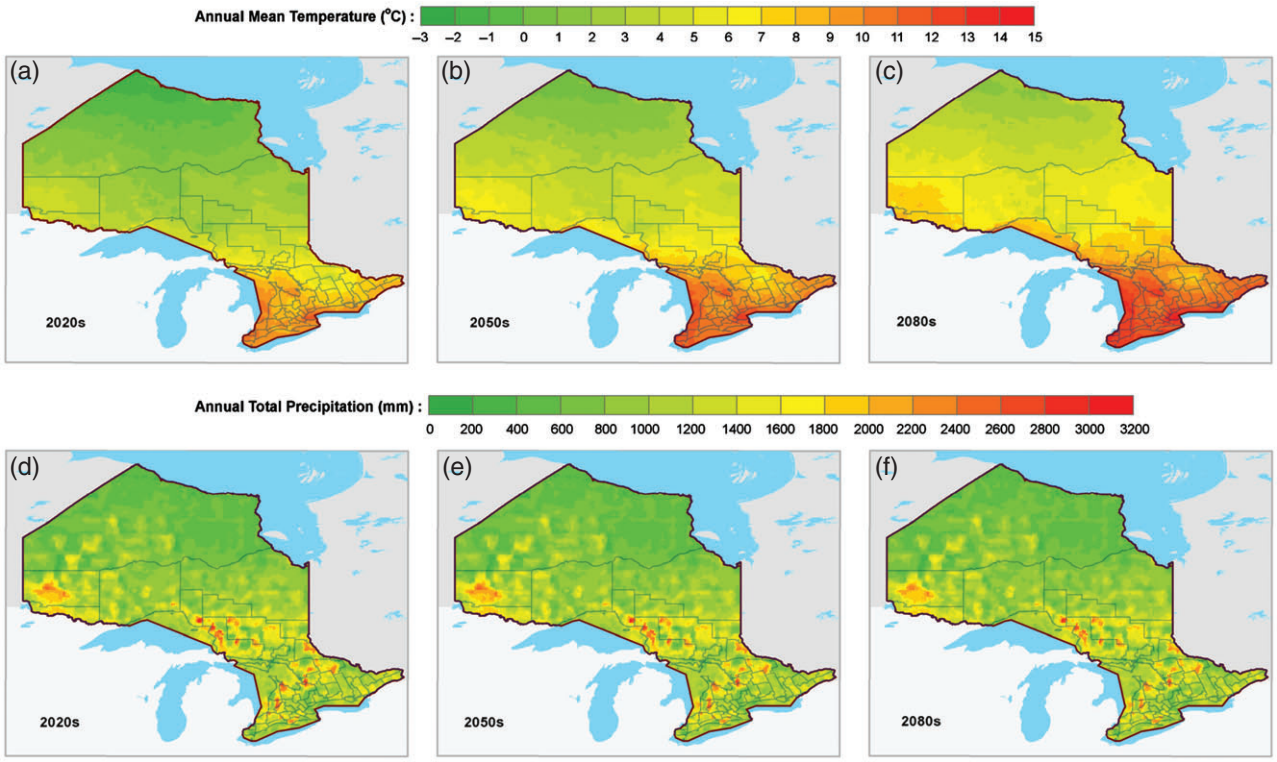

Figure 9. Maps of projected high-resolution (a–c) annual mean temperature and (d–f) annual total precipitation over Ontario, for three 30-year time periods (a,d) 2020s, (b,e) 2050s, and (c,f) 2080s.

Acknowledgements

The high-resolution projections for the province of Ontario generated in this research are available at http://env.uregina.ca/moe/ds (accessed 20 July 2014). We thank the UK Met Office Hadley Centre for providing the boundary conditions for our PRECIS experiments. This research was supported by the Natural Sciences Foundation (No. 51190095), the 111 Project (No. B14008), Ontario Ministry of the Environment, and the Natural Science and Engineering Research Council of Canada.

References

Beckmann BR, Adri Buishand T. 2002. Statistical downscaling relationships for precipitation in the Netherlands and North Germany. *Int. J. Climatol.* **22**: 15–32.

Charles SP, Bates BC, Smith IN, Hughes JP. 2004. Statistical downscaling of daily precipitation from observed and modelled atmospheric fields. *Hydrol. Processes* **18**: 1373–1394.

Chen D, Chen Y. 2003. Association between winter temperature in China and upper-air circulation over East Asia revealed by canonical correlation analysis. *Global Planet. Change* **37**: 315–325.

Chen J, Brissette FP, Leconte R. 2012. Coupling statistical and dynamical methods for spatial downscaling of precipitation. *Clim. Change* **114**: 509–526.

Cleveland WS. 1979. Robust locally weighted regression and smoothing scatterplots. *J. Am. Stat. Assoc.* **74**: 829–836.

Crane RG, Hewitson BC. 1998. Doubled CO2 precipitation changes for the Susquehanna basin: down-scaling from the GENESIS general circulation model. *Int. J. Climatol.* **18**: 65–76.

Diez E, Primo C, Garcia-Moya J, Gutiérrez J, Orfila B. 2005. Statistical and dynamical downscaling of precipitation over Spain from DEMETER seasonal forecasts. *Tellus A* **57**: 409–423.

Feser F, Rockel B, von Storch H, Winterfeldt J, Zahn M. 2011. Regional climate models add value to global model data: A review and selected examples. *Bull. Am. Meteorol. Soc.* **92**: 1181–1192.

Fowler H, Blenkinsop S, Tebaldi C. 2007. Linking climate change modelling to impacts studies: Recent advances in downscaling techniques for hydrological modelling. *Int. J. Climatol.* **27**: 1547–1578.

Giorgi F, Hewitson B, Christensen J, Hulme M, von Storch H, Whetton P, Jones R, Mearns L, Fu C. 2001. Regional climate information – evaluation and projections. In *Climate Change 2001: The Scientific Basis. Contribution of Working Group to the Third Assessment Report of the Intergovernmental Panel on Climate Change*, Chapter 10, Houghton JT, Ding Y, Griggs DJ, Noguer M, van der Linden PJ, Dai X, Maskell K, Johnson CA. (eds.): 607–616. Cambridge University Press: Cambridge, UK and New York, NY.

Haylock MR, Cawley GC, Harpham C, Wilby RL, Goodess CM. 2006. Downscaling heavy precipitation over the United Kingdom: A comparison of dynamical and statistical methods and their future scenarios. *Int. J. Climatol.* **26**: 1397–1415.

Hellström C, Chen D. 2003. Statistical downscaling based on dynamically downscaled predictors: Application to monthly precipitation in Sweden. *Adv. Atmos. Sci.* **20**: 951–958.

Hellström C, Chen D, Achberger C, Raisanen J. 2001. Comparison of climate change scenarios for Sweden based on statistical and dynamical downscaling of monthly precipitation. *Clim. Res.* **19**: 45–55.

Hessami M, Gachon P, Ouarda TB, St-Hilaire A. 2008. Automated regression-based statistical downscaling tool. *Environ. Modell. Softw.* **23**: 813–834.

Hewitson B, Crane R. 1996. Climate downscaling: Techniques and application. *Clim. Res.* **7**: 85–95.

Hirsch RM, Slack JR, Smith RA. 1982. Techniques of trend analysis for monthly water quality data. *Water Resour. Res.* **18**: 107–121.

Huth R. 1999. Statistical downscaling in central Europe: Evaluation of methods and potential predictors. *Clim. Res.* **13**: 91–101.

Jones RG, Noguer M, Hassell DC, Hudson D, Wilson SS, Jenkins GJ, Mitchell JFB. 2004. *Generating High-Resolution Climate Change Scenarios Using PRECIS.* Met Office Hadley Centre: Exeter, UK.

Kendall M. 1970. *Rank Correlation Methods* (4th edn). Griffin: London.

Lavender S, Walsh K. 2011. Dynamically downscaled simulations of Australian region tropical cyclones in current and future climates. *Geophys. Res. Lett.* **38**: L10705, doi: 10.1029/2011GL047499.

Mann HB. 1945. Non-parametric test against trend. *Econometrika* **13**: 245–259.

Maraun D, Wetterhall F, Ireson AM, Chandler RE, Kendon EJ, Widmann M, Brienen S, Rust HW, Sauter T, Themessl M, Venema VKC, Chun KP, Goodess CM, Jones RG, Onof C, Vrac M, Thiele-Eich I. 2010. Precipitation downscaling under climate change: Recent developments to bridge the gap between dynamical models and the end user. *Rev. Geophys.* **48**: RG3003, doi: 10.1029/2009RG000314.

Mesinger F, DiMego G, Kalnay E, Mitchell K, Shafran PC, Ebisuzaki W, Jović D, Woollen J, Rogers E, Berbery EH, Ek MB, Fan Y, Grumbine R, Higgins W, Li H, Lin Y, Manikin G, Parrish D, Shi W. 2006. North American regional reanalysis. *Bull. Am. Meteorol. Soc.* **87**: 343–360.

Mullan D, Fealy R, Favis-Mortlock D. 2012. Developing site-specific future temperature scenarios for Northern Ireland: Addressing key issues employing a statistical downscaling approach. *Int. J. Climatol.* **32**: 2007–2019.

Nakićenović N, Swart R. (eds.) 2000. *Emission Scenarios: Summary for Policymakers. Special Report of Working Group III of the Intergovernmental Panel on Climate Change.* IPCC: Geneva, Switzerland.

NLWIS. 2008. 'A daily 10 km gridded climate dataset for Canada, 1961–2003'. http://www.lib.uwaterloo.ca/locations/umd/digital/documents/ClimateDatasetDaily10kmGrids.html (accessed 18 March 2014).

Pal JS, Giorgi F, Bi X, Elguindi N, Solmon F, Rauscher SA, Gao X, Francisco R, Zakey A, Winter J, Ashfaq M, Syed FS, Sloan LC, Bell JL, Diffenbaugh NS, Karmacharya J, Konaré A, Martinez D, da Rocha RP, Steiner AL. 2007. Regional climate modeling for the developing world: The ICTP RegCM3 and RegCNET. *Bull. Am. Meteorol. Soc.* **88**: 1395–1409.

Rhines PB. 1979. Geostrophic turbulence. *Annu. Rev. Fluid Mech.* **11**: 401–441.

Saha S, Moorthi S, Pan H-L, Wu X, Wang J, Nadiga S, Tripp P, Kistler R, Woollen J, Behringer D, Liu H, Stokes D, Grumbine R, Gayno G, Wang J, Hou Y-T, Chuang H-Y, Juang H-MH, Sela J, Iredell M, Treadon R, Kleist D, Van Delst P, Keyser D, Derber J, Ek M, Meng J, Wei H, Yang R, Lord S, Van Den Dool H, Kumar A, Wang W, Long C, Chelliah M, Xue Y, Huang B, Schemm J-K, Ebisuzaki W, Lin R, Xie P, Chen M, Zhou S, Higgins W, Zou C-Z, Liu Q, Chen Y, Han Y, Cucurull L, Reynolds RW, Rutledge G, Goldberg M. 2010. The NCEP climate forecast system reanalysis. *Bull. Am. Meteorol. Soc.* **91**: 1015–1057.

Salathé EP. 2003. Comparison of various precipitation downscaling methods for the simulation of streamflow in a rainshadow river basin. *Int. J. Climatol.* **23**: 887–901.

Semenov MA, Barrow EM. 1997. Use of a stochastic weather generator in the development of climate change scenarios. *Clim. Change* **35**: 397–414.

Sen PK. 1968. Estimates of the regression coefficient based on Kendall's tau. *J. Am. Stat. Assoc.* **63**: 1379–1389.

Timbal B, Fernandez E, Li Z. 2009. Generalization of a statistical downscaling model to provide local climate change projections for Australia. *Environ. Modell. Softw.* **24**: 341–358.

Van Vuuren DP, Edmonds J, Kainuma M, Riahi K, Thomson A, Hibbard K, Hurtt GC, Kram T, Krey V, Lamarque J-F, Masui T, Meinshausen M, Nakićenović N, Smith SJ, Rose SK. 2011. The representative concentration pathways: An overview. *Clim. Change* **109**: 5–31.

Wang X, Huang G, Lin Q, Nie X, Cheng G, Fan Y, Li Z, Yao Y, Suo M. 2013. A stepwise cluster analysis approach for downscaled climate projection – A Canadian case study. *Environ. Modell. Softw.* **49**: 141–151.

Wang X, Huang G, Lin Q, Liu J. 2014. High-resolution probabilistic projections of temperature changes over Ontario, Canada. *J. Clim.* **27**: 5259–5284.

White CJ, McInnes KL, Cechet RP, Corney SP, Grose MR, Holz GK, Katzfey JJ, Bindoff NL. 2013. On regional dynamical downscaling for the assessment and projection of temperature and precipitation extremes across Tasmania, Australia. *Clim. Dyn.* **41**: 3145–3165.

Wilby RL, Wigley TML. 2000. Precipitation predictors for downscaling: observed and general circulation model relationships. *Int. J. Climatol.* **20**: 641–661.

Wilby RL, Dawson CW, Barrow EM. 2002. SDSM – a decision support tool for the assessment of regional climate change impacts. *Environ. Modell. Softw.* **17**: 145–157.

Wilby R, Charles S, Zorita E, Timbal B, Whetton P, Mearns L. 2004. 'Guidelines for use of climate scenarios developed from statistical downscaling methods'.

Wilson S, Hassell D, Hein D, Morrell C, Tucker S, Jones R, Taylor R. 2011. *Installing and Using the Hadley Centre Regional Climate Modelling System, PRECIS (Version 1.9.3)*. Met Office Hadley Centre: Exeter, UK.

Zhang Y, Xu Y, Dong W, Cao L, Sparrow M. 2006. A future climate scenario of regional changes in extreme climate events over China using the PRECIS climate model. *Geophys. Res. Lett.* **33**: L24702, doi: 10.1029/2006GL027229.

Zhu C, Lettenmaier DP, Cavazos T. 2005. Role of antecedent land surface conditions on North American monsoon rainfall variability. *J. Clim.* **18**: 3104–3121.

